International Journal of Power Electronics and Drive System (IJPEDS)
Vol. 12, No. 2, Jun 2021, pp. 772~782
ISSN: 2088-8694, DOI: 10.11591/ijpeds.v12.i2.pp772-782

Detailed analysis of grid connected and islanded operation modes based on P/U and Q/f droop characteristics

Qusay Salem[1], Khaled Alzaareer[2]
[1]Department of Electrical Engineering, Princess Sumaya University for Technology, Jordan
[2]Department of Electrical Engineering, Quebec University, Montreal Québec, Canada

Article Info

Article history:

Received Dec 30, 2020
Revised Apr 7, 2021
Accepted Apr 20, 2021

Keywords:

Distributed generators
Droop control
Grid connected and Islanded Modes
Microgrid
Voltage source inverter

ABSTRACT

This paper presents a thorough control structure of the distributed generators inside the microgrid during both grid-connected and islanded operation modes. These control structures of the DGs voltage source inverters are implemented in synchronous reference frame (SRF) and controlled using linear PI controllers. By implementing the control structures, the desired real and reactive power can be efficiently transferred to the local loads and the utility load by the microgrid generating units. A modified droop control technique is introduced to facilitate the microgrid performance during both modes of operation. The active and reactive power sharing of the load demand between the utility grid and the microgrid can be performed by this droop control technique during the islanded mode. The system performance during intentional islanding event and utility load increase is investigated. The effectiveness of the offered control structures is confirmed through simulation results during both modes of operation.

Corresponding Author:

Qusay Salem
Department of Electrical Engineering
Princess Sumaya University for Technology
Amman, Jordan
Email: q.salem@psut.edu.jo

1. INTRODUCTION

Microgrids are energy networks which have small-scale and low-voltage feature. They are utilized to guarantee the distribution and generation locally in the autonomous or remote societies [1]. Microgrids can be interconnected with large power systems through power electronic converters and can even work autonomously [2], [3]. In the normal operation where the microgrid is connected to the massive grid, DGs into the power network can track the grid energy flow and operate without control requirment. In the event of short circuit or planned interruption, the microgrid can be disconnected from the large grid to operate in autonomous mode where proper control methods are applied in order to ensure stability of power [4], [5]. The autonomous functionality can provide more elacticity to the DGs involvement and bring a more efficient power supply. However, autonomous microgrids might have powerless condition than conventional massive grids because of limited capacities of the DGs [6].

The microgrid notion advocates coordinated control where retrieving trustworthy and high-quality energy can be ensured to customers by DGs cooperation [7]. The controlled voltage source converters-based power electronic interfaces are utilized widely to connect the DGs to the point of common coupling of the network. Moreover, two main categories of microgrid control methods are existed which are divided into either centralized control or decentralized control methods [8]-[10]. A high bandwidth communication link is employed in centralized control methods to transfer feedback and control signals between the centralized

controller and the DGs. Centralized controllers are found to be less reliable since system instability might appear due to any communication interruption beside the communication system higher costs [11]-[14]. That's why decentralized control methods are considered more feasible as performing the system online maintenance and achieving self-organizing can be accomplished easily [15], [16]. The methods of decentralized control employ $P-f$ & $Q-E$ droop characteristics to regulate the flow of real and reactive power in the microgrid. These droop characteristics are based on highly inductive networks where the decoupling of real and reactive power flow equations can be applied. Slow dynamics and voltage drifts with load change are some features of these droop characteristics which are compatbile with the network impedance high X/R ratio and large inertia in conventional power systems [17], [18]. However, since line impedances in microgrids are resistive at most, DGs have small inertia and persistent load variations may happen. The X/R ratio in microgrids is not large like the case in conventional power systems. Consequently, the active and reactive power flow is dependent on δ and E as they are highly coupled. That's why the traditional droop technique which employs decoupled $P-f$ & $Q-E$ droops bring out weak performance. Different controllers have been proposed in this context where [19] introduces a virtual resistance so that the system acts in a resistive manner where P and Q might be regulated by respectively drooping E and f. [20] and [21] have introduced a virtual reactance and a virtual PQ method, respectively to mimic the inductive system by increasing the X/R ratio. The $P-f$ & $Q-E$ droop scheme has the disadvantage of exhibiting power quality problems in terms of frequency and voltage deviations. Replacing the $P-f$ droop by $P-\delta$ droop can eliminate the frequency deviations problem where a global positioning system is introduced to synchronize the DG units [22]. E. Rokrok and M. Golshan [23] have introduced an adaptive voltage droop method for improving the regulation of voltage at PCC and mitigating the coupling between P and Q droop controllers. In [24], synchronizing the global frequency to a nominal value with better disturbance rejection properties has been realized by considering a finite-time control protocol for frequency restoration, based on feedback linearization. DG self-frequency restoration control has corrected the frequency deviation by droop compensation without the need of utilizing a secondary controller [25]. However, resistive line impedance in low voltage microgrids causes power coupling in $P-f$ droop control which hasn't been considered and was only applied to high or medium voltage networks.

The current communication-less microgrid control methods have utilized $P-f$ & $Q-E$ droop characteristics. An alternative approach is proposed in this paper where a $P-U$ and $Q-f$ droop control technique is proposed for a microgrid connected to the utility or main grid. The control structures that are implemented to execute the grid-connected and islanded operations of DGs are investigated. An intentional islanding condition is performed to investigate the performance of the microgrid control structures. Moreover, a step change in the utility load has been proposed to prove the control structures performance. The proposed control strategies can control the voltage and power of the DGs in addition to sharing the load demand during all modes of operation. The main contribution of this work is accomplished by considering the abovementioned issues.

The organization of the paper is divided into five sections. At first is the introduction, then section 2 presents the general schematic diagram of the proposed microgrid model. The real and reactive power generation in relation to the proposed droop control methodology is introduced in section 3. Section 4 shows the simulation results which are performed to confirm the applicability and efficiency of the proposed control structures. Finally, section 5 presents the conclusion of the proposed work.

2. THE PROPOSED NETWORK DESCRIPTION

Figure 1 shows a single-line diagram of the proposed microgrid model which can operate in grid connected and islanded modes. All the distributed generators are supposed to inject the required active and reactive power to support their own loads and the utility load then the remnant of power moves out to the main utility grid. A circuit breaker is placed in the system either to maintain the microgrid online with the main grid or to isolate the faulty sections from the microgrid in case of short circuits. A utility load is connected directly to the point of common coupling (PCC) to be supported by real and reactive power in both modes of operation.

2.1. Modeling and control of grid-connected DC/AC voltage source inverter

Variables in synchronous reference frame (SRF) are used for the control of grid connected inverters in which they described as DC quantities. Figure 2 depicts the circuit diagram of the three-phase voltage source inverter connected to the grid. Ua, Ub, Uc are the inverter output voltages, Ea, Eb, Ec are the output voltages of the grid. The inductance of the inverter is denoted by Li and Lg is the inductance of the grid. ia, ib, ic are the injected currents in the main grid.

The equation of the diagram depicted in Figure 2 is formulated differentially as:

$$L[\frac{di}{dt}]_{abc} = [U]_{abc} - [E]_{abc} - R[i]_{abc} \quad (1)$$

Where, the total inductance of the inverter is denoted by L, which means $L = Li + Lg$. If $\omega = 2\pi f$, where ω is the frequency of the grid, then (1) can be formulated in synchronous reference frame as:

$$U_{dq,ref} = L\frac{di_{dq}}{dt} + (R + j\omega L)i_{dq} + U_{dq} \quad (2)$$

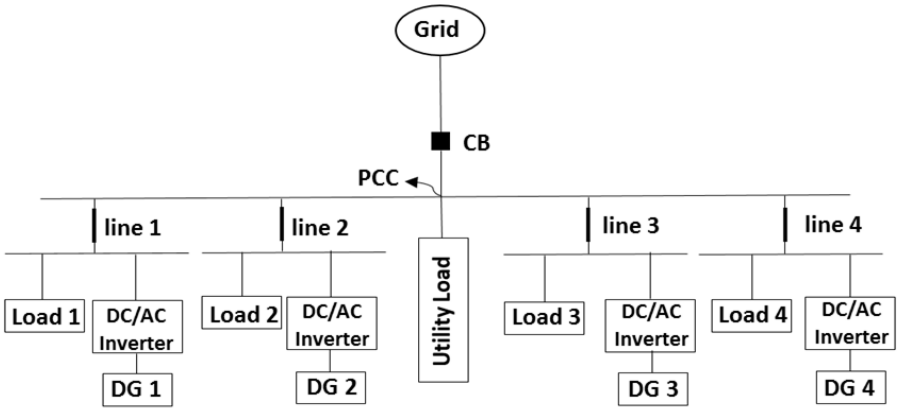

Figure 1. The proposed microgrid model

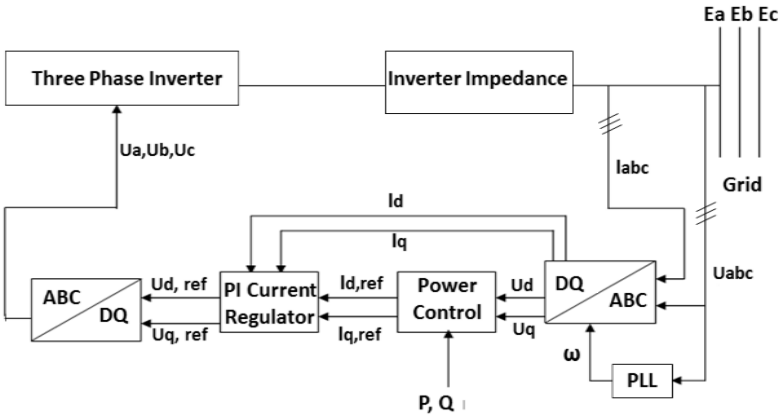

Figure 2. Three phase DC/AC voltage source converter connected to grid

Then the real part and the imaginary part of (2) can be written as:

$$U_{d,ref} = L\frac{d_{id}}{dt} + Ri_d - \omega Li_q + U_d \quad (3)$$

$$U_{q,ref} = L\frac{d_{iq}}{dt} + Ri_q + \omega Li_d + U_q \quad (4)$$

Depending on (3) and (4) the arrangement of the grid connected voltage source inverter current control in dq-reference frame is illustrated as shown in Figure 3. Where, $i_{d,ref}, i_{q,ref}$ are the dq reference currents. A PLL is used for tracking the phase angle of the grid to be synchronized with DGs. PI controllers are used to compensate the voltage drop caused by the line impedance.

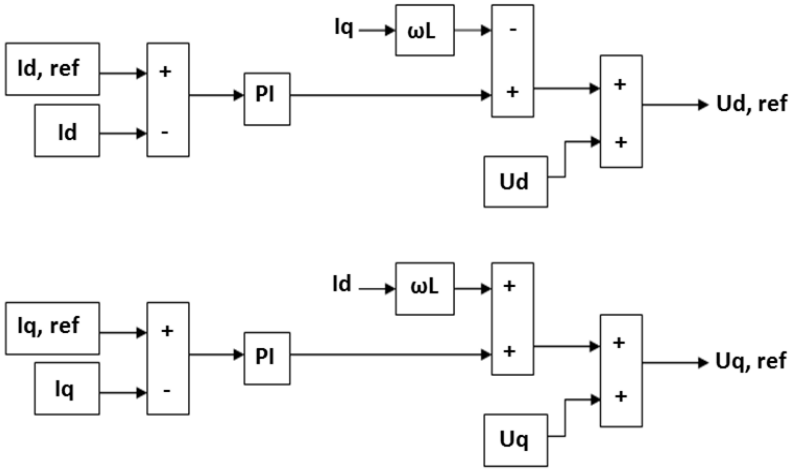

Figure 3. Block diagram of VSI current control

The control equations for $U_{d,ref}$ and $U_{q,ref}$ are as the following:

$$U_{d,ref} = U_d - \omega L i_q + \left(k_p + \frac{k_i}{s}\right)\left(i_{d,ref} - i_d\right) \quad (5)$$

$$U_{q,ref} = U_q - \omega L i_d + \left(k_p + \frac{k_i}{s}\right)\left(i_{q,ref} - i_q\right) \quad (6)$$

Hence, the formulas of active and reactive power are written in synchronous reference frame as:

$$P = \frac{3}{2}\left(U_{d,ref}\, i_d + U_{q,ref}\, i_q\right) \quad (7)$$

$$Q = \frac{3}{2}\left(U_{d,ref}\, i_q - U_{q,ref}\, i_d\right) \quad (8)$$

It can be seen from (7) and (8) that a mutual coupled voltage exists between the d and q axis quantities. However, this coupling will not cause independent control of P and Q. In other words, if the delivered real power changes, the reactive power will change accordingly. The elimination of this mutual coupling is achieved by considering $U_{q,ref} = 0$. Hence, the modified real and reactive power can be written as:

$$P = \frac{3}{2} U_{d,ref}\, i_d \quad (9)$$

$$Q = \frac{3}{2} U_{d,ref}\, i_q \quad (10)$$

Consequently, the d-axis current monitors directly the active power and the q-axis current monitors the reactive power.

2.2. Control of DC/AC voltage source inverter in islanded mode

Once the main utility grid is seperated from the microgrid, every DG inside the microgrid will lose stability in terms of very high values of current or voltage transients. In island mode, the grid feeding power converters can not work unless if a grid forming or grid supporting power converter is existed so that the voltage amplitude and frequency of the ac microgrid can be adjusted [26]. In this paper, a power converter which is grid forming one is activated at PCC when the microgrid becomes islanded. The circuit diagram of the grid forming power converter in islanded mode is depicted in Figure 4.

The reference values of the frequency and voltage is determined by a reference sinewave generator. This is because the microgrid has no physical connection with the main grid. Thus, the DG reference voltage in islanded mode is extracted as:

$$\left\{\begin{array}{c} U_a = E\sin(\omega t) \\ U_b = E\sin(\omega t - \frac{2\pi}{3}) \\ U_c = E\sin(\omega t + \frac{2\pi}{3}) \end{array}\right\} \quad (11)$$

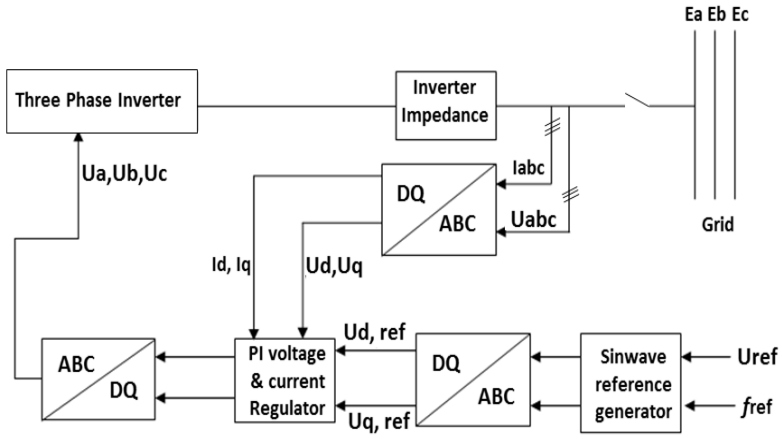

Figure 4. Circuit diagram of grid forming power converter in islanded mode

The voltage and current control circuit for the grid forming power converter in islanded mode is shown in Figure 5. In the islanded mode, the existing control acts as voltage control through compensation of current. The control unit employs voltage regulators to extract the desired current references. After that, using proper PI controllers, U_d and U_q will successfully track their references. The output current references $i_{d,ref}$ and $i_{q,ref}$ are compared with i_d and i_q, and the difference is inserted to another PI controller. Finally, the resultant output of the current loop performs as a voltage reference signal which is delivered to the gating signals of the three-phase power converter.

3. REAL AND REACTIVE POWER BASED ON DROOP CONTROL TECHNIQUE

Giving consideration to the converter as a voltage source which is controllable and taking into account that the converter is attached to the main grid via a line impedance as illustrated in Figure 6 (a), then the transmitted real and reactive power to the main grid can be formulated as:

$$P_A = \frac{U_A}{R^2+X^2}[R(U_A - U_b\,cos\delta) + XU_B sin\delta] \quad (12)$$

$$Q_A = \frac{U_A}{R^2+X^2}[-R(U_B\,sin\delta) + X(U_A - U_B cos\delta)] \quad (13)$$

Where, the real and reactive power passing to the grid from the power converter are denoted by P_A and Q_A, the voltages of the two power converters are denoted by U_A, U_b, the phase angle difference between both converter voltages is denoted by δ, the line impedance is denoted by $Z = R + jX$ and the impedance angle is denoted by φ. Thus, as $R = Z.cos\varphi$ and $X = Z.sin\varphi$, the vector representation of the given model can be represented in Figure 6 (b).

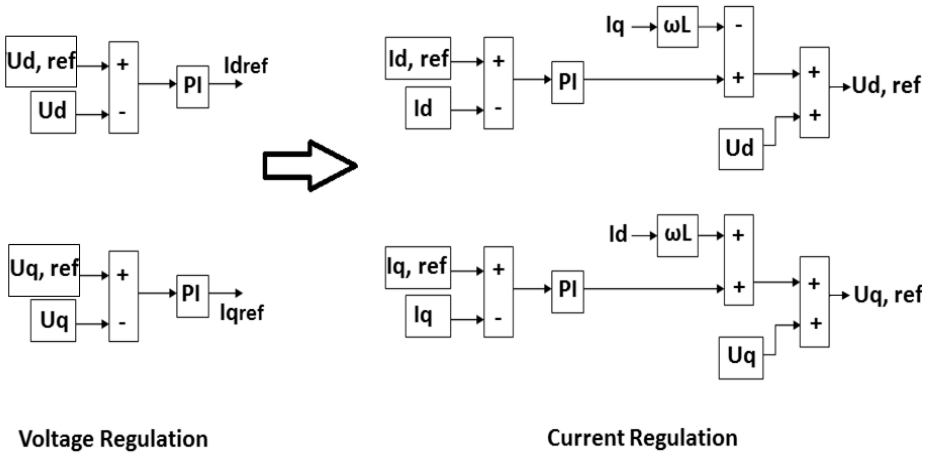

Figure 5. Voltage and current control of the power converter in the islanded mode

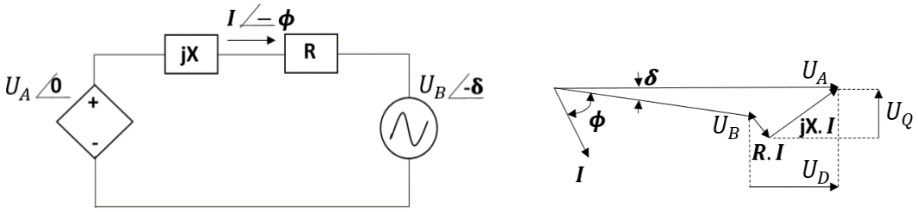

(a) (b)

Figure 6. Modelling of power converter connected to the distribution network, (a) equivalent circuit (b) phasor diagram

In low-voltage networks, the impedance of the grid is principally resistive and thus the inductive part can approximately be neglected. If we assume a small value of the phase angle δ, then (12) and (13) can be rewritten as:

$$P_A = \frac{U_A}{R}(U_A - U_B cos\delta) \Rightarrow U_A - U_B \approx \frac{RP_A}{U_A} \quad (14)$$

$$Q_A = -\frac{U_A \cdot U_B}{R} sin\delta \Rightarrow \delta = -\frac{RQ_A}{U_A U_B} \quad (15)$$

Based on the previous two equations, it can be noticed that the voltage magnitude in low-voltage distribution networks and the real power are dependent to each other. Also, the reactive power and the frequency are influenced by each other. From (14) and (15), the expressions of the droop control are demonstrated as:

$$U - U_o = -k_p(P - P_o) \quad (16)$$

$$f - f_o = k_q(Q - Q_o) \quad (17)$$

The characteristics of the proposed droop control are illustrated in Figure 7. The characteristics demonstrate that the voltage magnitude and the active power are mainly dependent. On the other hand, it is clear that the frequency and the reactive power are also dependent on each other.

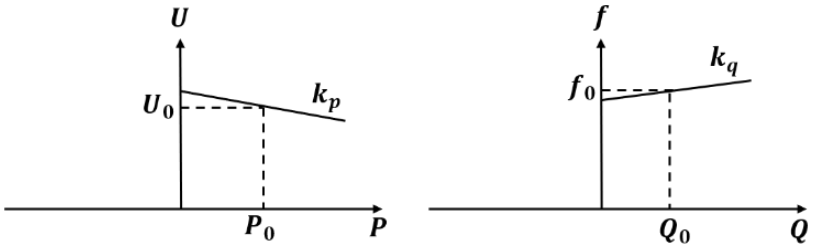

Figure 7. P/U and Q/f droop control characteristics

4. DISCUSSION OF SIMULATION RESULTS

Realization and robustness of the proposed droop control strategies in the microgrid model have been assessed in steady state and transient operating conditions employing 'SimPowerSystems' library toolbox in Matlab/Simulink. The parameters of the single line diagram shown in Figure 1 are given in Table 1. Two scenarios have been evaluated through simulations to examine the system behavior. The first scenario is when an intentional islanding condition takes place. The other scenario is when the utility load increases during the islanding period. The significance and novel aspects of the results are obvious by the operation of the proposed droop control technique where the DGs share the real power to fulfill the total load demand for both scenarios. Moreover, the obtained results reflect the stability and solidity of the DG VSI control strategy during both grid-connected and islanded operation modes.

Table 1. Parameters of the proposed model

Grid	$Vrms = 230\,V, f = 50\,Hz$
DG 1	$P = 12\,kw, Q = 4\,kvar$
DG 2	$P = 14\,kw, Q = 6\,kvar$
DG 3	$P = 16\,kw, Q = 8\,kvar$
DG 4	$P = 18\,kw, Q = 10\,kvar$
Utility Load	$P = 30\,kw, Q = 5\,kvar$
DGs Loads	$P = 5\,kw, Q = 0\,kvar$
Line impedance	$R = 0.5\,\Omega, L = 0.8\,mH$

4.1. Intentional islanding scenario

The microgrid is assumed to work in grid-connected mode at $(0 \leq t \leq 1)$ and then disconnected from the utility following an intentional islanding condition at PCC which is proposed at $t = 1s$ and lasts for $1000ms$ $(1 \leq t \leq 2)$. After that the system regains its operation to relate to the main grid at $(2 \leq t \leq 3)$. Figure 8 (a)-(d) depicts the microgrid performance concerning the real power, reactive power, rms voltage and frequency while subfigures (e)-(h) depict the grid performance in terms of real power, rms voltage, current and frequency.

It is noticed from the results that the proposed droop control strategies are functioning effectively during grid-connected and islanded modes. Furthermore, it can be noticed that when islanding occurs, the DGs share the real power to fulfill the total load demand since the power supply of the main grid is lost. As a result, the rms voltage of the DGs inverters is increased based on the droop characteristics. The reactive power and frequency of DGs inverters show a little transient at the time of islanding and reconnection due to the circuit breaker operation. At the grid side, it can be noticed that the system is completely islanded at $(1 \leq t \leq 2)$ as the grid real power and current reach zeros. In addition, it is also noticed that a small fluctuation on grid frequency is existed at the time of islanding and reconnection conditions. Every DG in the microgrid is equipped with identical droop characteristic is applied for where the DGs real power are shared equally to satisfy the local loads and the utility load during the islanding period $(1 \leq t \leq 2)$.

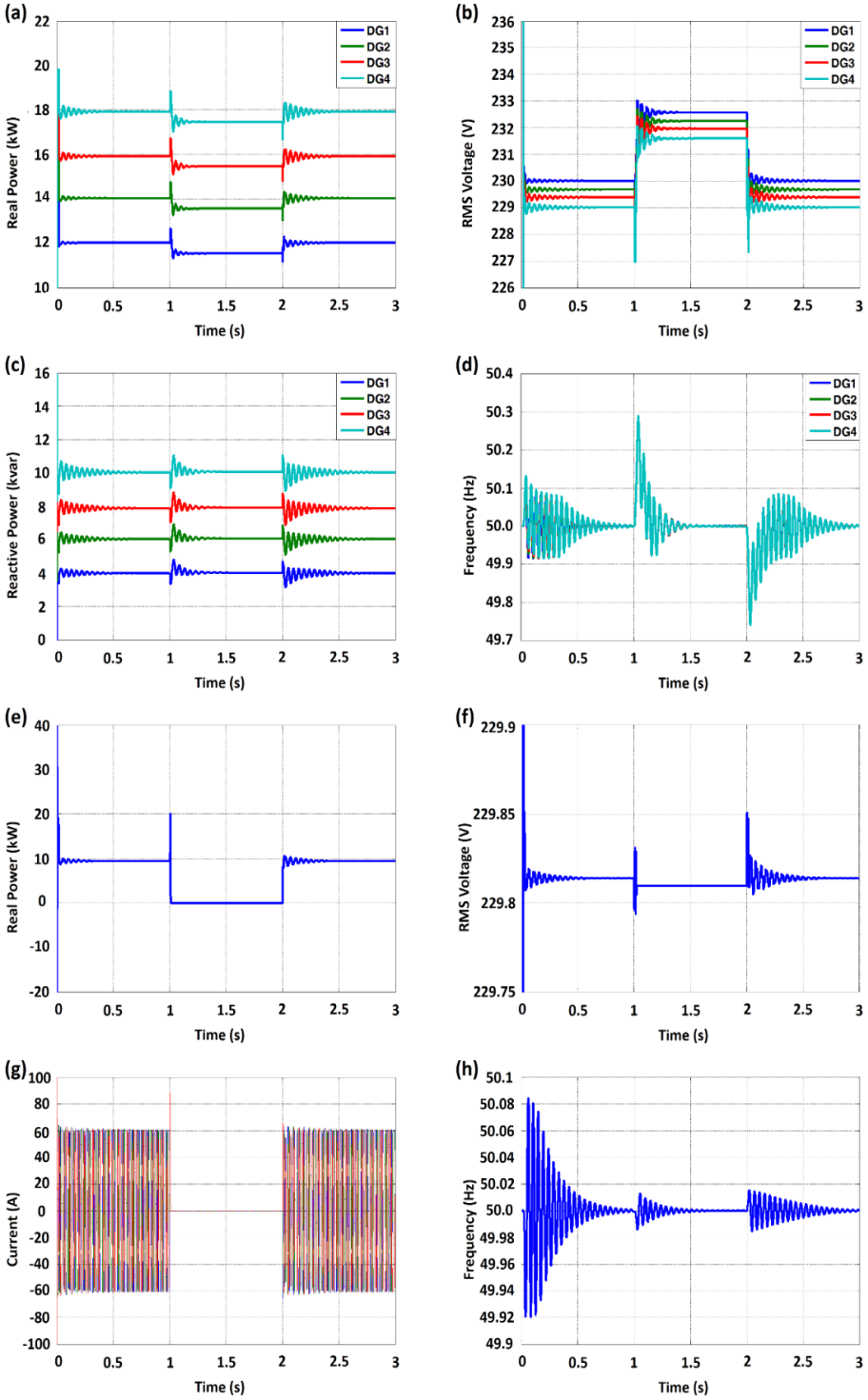

Figure 8. Microgrid and grid performance during intentional islanding scenario

4.2. Utility load increase scenario

Figure 9 (a)-(d) shows the behavior of the microgrid when the utility load increases. The utility load has been increased from 30kw to 50 kw in order to investigate the performance of real and reactive power sharing between the grid and microgrid especially when the system is islanded. It is clearly shown that the real power of DGs inverters in islanding mode have increased to compensate the shortage of generation from the main grid in order to support the demand of utility load. Again, identical droop characteristics are applied

for each DG to satisfy the increase in the utility load during the islanding period. This was done by sharing the real power of all DGs such that the utility load increase is divided on the four DGs equally.

Consequently, the DGs rms voltage has decreased based on the droop characteristics. The reactive power and frequency of DGs remain as before with a little transient at the time of islanding and reconnection. However, it can be seen from subfigures (e)-(h) that the main grid real power and current approaches zero as a result of the islanding condition while the voltage and frequency remain within their permissible limits during both grid connected and islanded modes.

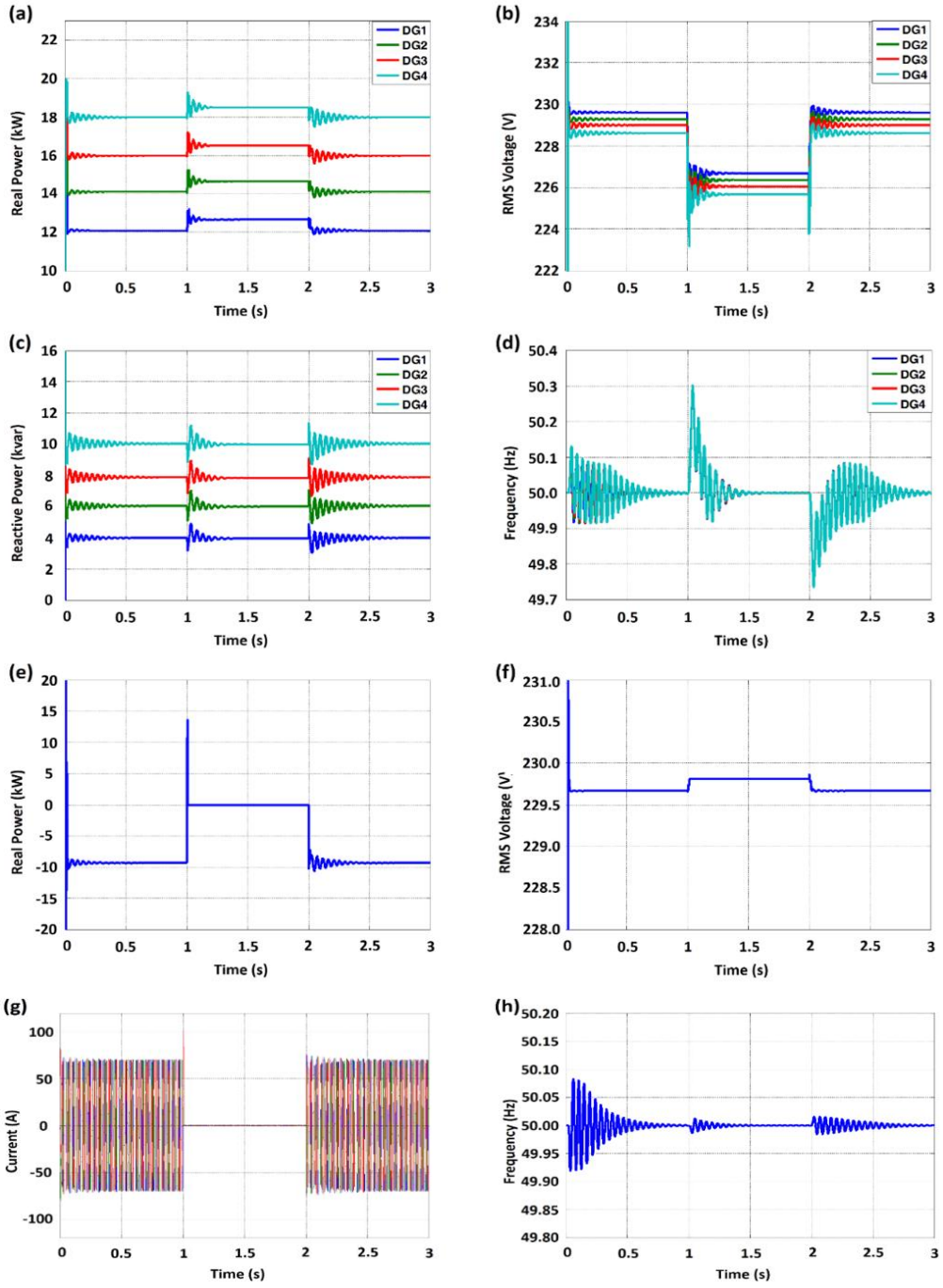

Figure 9. Microgrid and grid performance during utility load increase scenario

5. CONCLUSION

The system efficacy and behavior of the proposed droop control have been investigated during both grid-connected and islanded modes by proposing an intentional islanding condition at PCC and by increasing of the utility load. Two control interfaces are employed to design the control strategies, the first one represents the grid connected mode and the other one represents the islanded mode. The simulation results confirmed that the response of the proposed control strategies and the droop control can maintain the system parameters within acceptable limits during both modes of operation. The addition of anti-islanding algorithms or techniques to the control units of the microgrid is a proper path of the future work.

REFERENCES

[1] C.-S. Karavas, G. Kyriakarakos, K. Arvanitis and G. Papadakis, "A multi-agent decentralized energy management system based on distributed intelligence for the design and control of autonomous polygeneration microgrids," *Energy Conversion and Management* , vol. 103, pp. 166-179, 2015, DOI: 10.1016/j.enconman.2015.06.021.

[2] J. Li, Y. Liu and L. Wu, "Optimal Operation for Community-Based Multi-Party Microgrid in Grid-Connected and Islanded Modes," *IEEE Transactions on Smart Grid,* vol. 9, no. 2, pp. 756-765, 2018, doi: 10.1109/TSG.2016.2564645.

[3] H. Ali, A. Hussain, V. Bui and H. Kim, "Consensus Algorithm-Based Distributed Operation of Microgrids During Grid-Connected and Islanded Modes," *IEEE Access,* vol. 8, pp. 78151-78165, 2020, DOI: 10.1109/ACCESS.2020.2989457.

[4] C. Dou, Z. Zhang, D. Yue and H. Gao, "An Improved Droop Control Strategy Based on Changeable Reference in Low-Voltage Microgrids," *Energies* , vol. 10, pp. 1-18, 2017, DOI: 10.3390/en10081080.

[5] Q. Salem, L. Liu and J. Xie, "Dual Operation Mode of a Transformerless H-Bridge Inverter in Low-Voltage Microgrid," *IEEE Transactions on Industry Applications,* vol. 55, no. 5, pp. 5289-5299, 2019, DOI: 10.1109/TIA.2019.2917807.

[6] X. Wang, F. Blaabjerg and Z. Chen, "Autonomous Control of Inverter-Interfaced Distributed Generation Units for Harmonic Current Filtering and Resonance Damping in an Islanded Microgrid," *IEEE Transactions on Industry Applications,* vol. 50, no. 1, pp. 452 - 461, 2014, DOI: 10.1109/TIA.2013.2268734.

[7] M. S. Golsorkhi and D. D. C. Lu, "A Control Method for Inverter-Based Islanded Microgrids Based on V-I Droop Characteristics," *IEEE Transactions on Power Delivery,* vol. 30, no. 3, pp. 1196-1204, 2015, DOI: 10.1109/TPWRD.2014.2357471.

[8] E. Espina, J. Llanos, C. Burgos-Mellado, R. Cárdenas-Dobson, M. Martínez-Gómez and D. Sáez, "Distributed Control Strategies for Microgrids: An Overview," *IEEE Access,* vol. 8, pp. 193412-193448, 2020, DOI: 10.1109/ACCESS.2020.3032378.

[9] Q. Salem and J. Xie, "Decentralized power control management with series transformerless H-bridge inverter in low-voltage smart microgrid based P/V droop control," *International Journal of Electrical Power & Energy Systems,* vol. 99, pp. 500-515, 2018, DOI: 10.1016/j.ijepes.2018.01.047.

[10] Q. Salem and K. Alzaareer, "Fault ride-through capability with mutual inductance in low-voltage single-phase microgrid," *IETE Journal of Research,* 2020, DOI: 10.1080/03772063.2020.1800524.

[11] Y. K. e. al, "On the Secondary Control Architectures of AC Microgrids: An Overview," in IEEE Transactions on Power Electronics," *IEEE Transactions on Power Electronics,* vol. 35, no. 6, pp. 6482-6500, 2020.

[12] Q. Xu, J. Xiao, P. Wang and C. Wen, "A Decentralized Control Strategy for Economic Operation of Autonomous AC, DC, and Hybrid AC/DC Microgrids," *IEEE Transactions on Energy Conversion,* vol. 32, no. 4, pp. 1345-1355, 2017, DOI: 10.1109/TEC.2017.2696979.

[13] J. Wang, C. Jin and P. Wang, "A Uniform Control Strategy for the Interlinking Converter in Hierarchical Controlled Hybrid AC/DC Microgrids," *IEEE Transactions on Industrial Electronics,* vol. 65, no. 8, pp. 6188-6197, 2018, DOI: 10.1109/TIE.2017.2784349.

[14] S. Ansari, A. Chandel and M. Tariq, "A Comprehensive Review on Power Converters Control and Control Strategies of AC/DC Microgrid," *IEEE Access,* vol. 9, pp. 17998-18015, 2021, DOI: 10.1109/ACCESS.2020.3020035.

[15] I. U. Nutkani, P. C. Loh, P. Wang and F. Blaabjerg, "Decentralized Economic Dispatch Scheme With Online Power Reserve for Microgrids," *IEEE Transactions on Smart Grid,* vol. 8, no. 1, pp. 139-148, 2017, DOI: 10.1109/TSG.2015.2451133.

[16] A. Vaccaro, V. Loia, G. Formato, P. Wall and . V. Terzija, "A Self-Organizing Architecture for Decentralized Smart Microgrids Synchronization, Control, and Monitoring," *IEEE Transactions on Industrial Informatics,* vol. 11, no. 1, pp. 289-298, 2015, DOI: 10.1109/TII.2014.2342876.

[17] M. A. Awal, H. Yu, H. Tu, S. M. Lukic and I. Husain, "Hierarchical Control for Virtual Oscillator Based Grid-Connected and Islanded Microgrids," *IEEE Transactions on Power Electronics,* vol. 35, no. 1, pp. 988-1001, 2020, DOI: 10.1109/TPEL.2019.2912152.

[18] M. Naderi, Y. Khayat, Q. Shafiee, T. Dragicevic, H. Bevrani and F. Blaabjerg, "Interconnected Autonomous AC Microgrids via Back-to-Back Converters—Part I: Small-Signal Modeling," *IEEE Transactions on Power Electronics,* vol. 35, no. 5, pp. 4728-4740, 2020, DOI: 10.1109/TPEL.2019.2943996.

[19] J. M. Guerrero, J. Matas, L. G. d. Vicuna, M. Castilla and J. Miret, "Decentralized Control for Parallel Operation of Distributed Generation Inverters Using Resistive Output Impedance," *IEEE Transactions on Industrial Electronics,* vol. 54, no. 2, pp. 994-1004, 2007, DOI: 10.1109/TIE.2007.892621.

[20] Y. C. C. Wong, C. S. Lim, M. D. Rotaru, A. Cruden and X. Kong, "Consensus Virtual Output Impedance Control Based on the Novel Droop Equivalent Impedance Concept for a Multi-Bus Radial Microgrid," *IEEE Transactions on Energy Conversion*, vol. 35, no. 2, pp. 1078-1087, 2020, DOI: 10.1109/TEC.2020.2972002.
[21] M. Naderi, Q. Shafiee, F. Blaabjerg and H. Bevrani, "Low-Frequency Small-Signal Modeling of Interconnected AC Microgrids," *IEEE Transactions on Power Systems*, 2020, DOI: 10.1109/TPWRS.2020.3040804.
[22] R. Majumder, A. Ghosh, G. Ledwich and F. Zare, "Angle droop versus frequency droop in a voltage source converter based autonomous microgrid," in *2009 IEEE Power & Energy Society General Meeting*, 2009, pp. 1-8, DOI: 10.1109/PES.2009.5275987.
[23] E. Rokrok and M. Golshan, "Adaptive voltage droop scheme for voltage source converters in an islanded multibus microgrid," *IET Generation, Transmission & Distribution*, vol. 4, no. 5, pp. 562-578, 2010, DOI: 10.1049/iet-gtd.2009.0146.
[24] S. Zuo, A. Davoudi, Y. Song and F. L. Lewis, "Distributed Finite-Time Voltage and Frequency Restoration in Islanded AC Microgrids," *IEEE Transactions on Industrial Electronics*, vol. 63, no. 10, pp. 5988-5997, 2016, DOI: 10.1109/TIE.2016.2577542.
[25] Y.-S. Kim, E.-S. Kim and S.-I. Moon, "Distributed Generation Control Method for Active Power Sharing and Self-Frequency Recovery in an Islanded Microgrid," *IEEE Transactions on Power Systems*, vol. 32, no. 1, pp. 544-551, 2017, DOI: 10.1109/TPWRS.2016.2543231.
[26] J. Chen, F. Milano and T. O'Donnell, "Assessment of Grid-Feeding Converter Voltage Stability," *IEEE Transactions on Power Systems*, vol. 34, no. 5, pp. 3980-3982, 2019, DOI: 10.1109/TPWRS.2019.2920516.

BIOGRAPHIES OF AUTHORS

Qusay Salem has been awarded the PhD degree in Electrical Power and Energy Engineering from University of Ulm – Germany, in 2020. He received the B.Sc. and M.Sc. Degree both in Electrical Power Engineering from University of Mutah and Yarmouk University – Jordan, in 2009 and 2013, respectively. Currently, he serves as an Assistant Professor with the Department of Electrical Engineering at Princess Sumaya University for Technology. His research interests include power control and energy management in low-voltage smart microgrids, Islanding detection schemes, Series power flow controllers.

Khaled Alzaareer received the PhD degree in Electrical Engineering/ Power Systems from Quebec University (ETS), Montreal, QC, Canada in Dec. 2020. He also received the bachelor's and master's degrees in electrical power engineering from Yarmouk University, Irbid, Jordan, in 2010 and 2012, respectively. His research interests are smart grid, sensitivity analysis, renewable energy integration, voltage stability and control.